ACS OMEGA

Article

Cite This: ACS Omega 2020, 5, 799−807

# Synergistic Fire Hazard Effect of a Multifunctional Flame Retardant in Building Insulation Expandable Polystyrene through a Simple Surface-Coating Method

Lin Li,*,† Xiaoming Shao,† Zheng Zhao, Xiaolin Liu, Licong Jiang, Kai Huang, and Shuai Zhao*

Key Lab of Rubber-plastics, Ministry of Education/Shandong Provincial Key Lab of Rubber-plastics, School of Polymer Science and Engineering, Qingdao University of Science and Technology, Qingdao 266042, China

**ABSTRACT:** This work reports a strategy based on γ-aminopropyltriethoxysilane (KH550) and graphene oxide (GO)-functionalized 9,10-dihydro-9-oxa-10-phosphaphenanthrene-10-oxide (DOPO) to fabricate P−N−Si integrated flame retardant [KDOPO-modified GO (DGO)] through mild Mannich and Silanization reactions to overcome the challenge of single gas-phase fire retardancy of DOPO. DGO-based phenolic epoxy resin (DGO/PER) is manufactured and coated on the surface of expandable polystyrene (EPS) foam plates to achieve fire safety, which is used as the thermally insulating external wall in buildings and constructions. The DGO/PER paintcoat imparts high fire safety to the EPS foam plate, exhibiting a high limiting oxygen index value of 29%, and a UL-94 V-0 classification is achieved with only 300 μm of layer thickness compared with the DOPO/PER paintcoat. Meanwhile, all combustion parameters such as peak heat release rate, heat release rate, total heat release, smoke release rate, total smoke rate, and ignition time present excellent promotions for EPS@DGO compared with EPS@DOPO. These dramatically reduced fire hazards are mainly attributed to the synergistic effects of DGO. Meanwhile, the DGO/PER flame-retardant paintcoat cannot deteriorate the thermal insulation performance of the EPS foam plate.

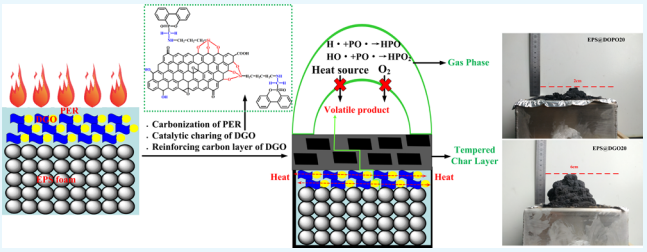


## INTRODUCTION

Presently, expandable polystyrene (EPS) foam has been extensively applied in construction, packing materials, cushioning, marine, and automobile because of its appealing features such as excellent thermal insulation properties, shock absorption, noise reduction properties, moisture resistance, good chemical resistance, convenience of processing, light weight, low cost, and so forth.[1−3] However, EPS foam is extremely flammable because of its interior beehive structure with large surface areas, and abundant toxic smoke may be released during combustion because of the existence of benzene in the molecule.[4,5] Therefore, it is imperative to improve the flame-resistance properties of EPS foams to ensure the safety of people's lives and properties. Nowadays, flame retardation of EPS foams is mainly achieved in the industry by halogen-containing flame retardants. Nevertheless, these halogenated flame retardants are now considered global pollutants with adverse effects on animal and human health.[6−8] Therefore, halogen-free flame retardation for EPS foams is an urgent issue. Among the "greener" halogen-free flame retardants, silicon, phosphorus, and/or nitrogen are the most popular elements.[9−14] Recently phosphorus flame retardants have been widely investigated because they can catalyze char formation in the condensed phase and/or capture active radicals in the gas phase.[15−17] Among these phosphorus flame retardants,[18] reactive flame retardant 9,10-dihydro-9-oxa-10-phosphaphenanthrene-10-oxide (DOPO) and its derivatives have attracted more and more attention because of their high thermal stability, good oxidation, and water resistance due to their stable aromatic structure.[19,20] However, since it is impossible to form a carbon layer after combustion, the main function of DOPO derivatives is to suppress the flame into the gas phase.[21] In order to improve their flame retardancy, DOPO derivatives with P−C, P−N, and P−O bond functions have been developed.[22−25] However, their high flame-retardant efficiency is usually achieved by a high flame-retardant loading. Nevertheless, based on the manufacturing process, flame-retardant EPS foams can be mainly obtained through adding a flame retardant in the polymerization stage and foaming process. Unfortunately, the additive of a flame retardant may seriously interfere with polymerization, leading to high residual styrene concentrations, and also affect the foaming process because of the diversity of flame retardants.[26,27] Recently, the microencapsulation method with halogen-free flame retardants has become a promising way to protect materials against fire because of the simplicity of processing.[28,29] For this method, the adhesion between the flame retardant and the EPS surface is a key problem to be considered. The commonly used binders are thermosetting phenolic resins and epoxy resins because of their inherent fire

Received: October 22, 2019
Accepted: December 18, 2019
Published: January 2, 2020




DOI: 10.1021/acsomega.9b03541
ACS Omega 2020, 5, 799−807

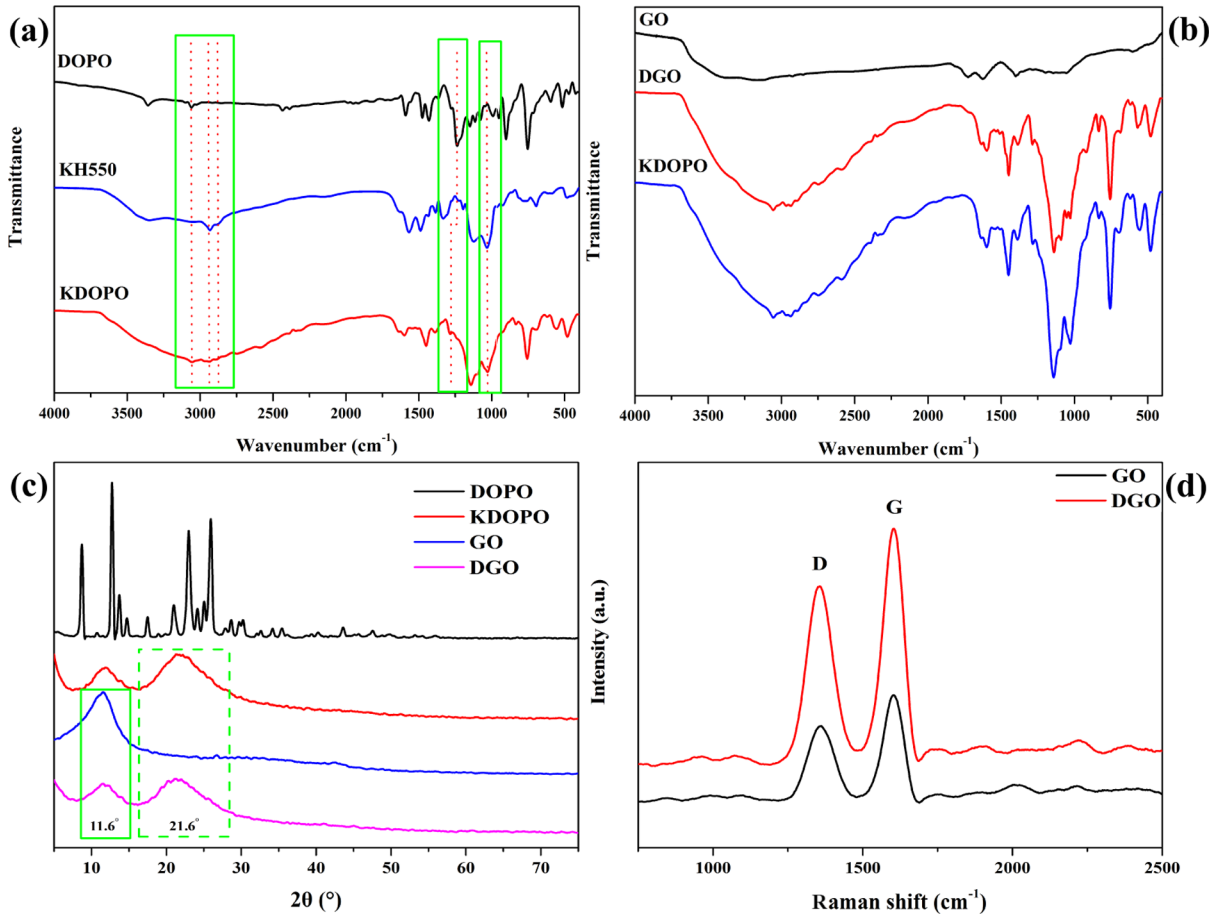


**Figure 1.** (a) FT-IR spectra of DOPO, KH550, and KDOPO; (b) FT-IR spectra of GO, KDOPO, and DGO; (c) XRD patterns of DOPO, GO, KDOPO, and DGO; (d) Raman patterns of GO and DGO.

resistance after curing and their good compatibility with EPS beads and inorganic fillers.[30] However, curing techniques of thermosetting resins are usually difficult to coordinate with the foaming techniques of EPS. Even though they can proceed simultaneously, the curing process of thermosetting resins also interferes with the foaming process of EPS more or less. Layer-by-layer (LbL) assembly is considered as another versatile and cost-effective strategy to construct a fire protection coating for material substrates.[31,32] In particular, LbL technique has been involved in constructing flame-retardant coating directly toward EPS foams, which avoids interfering with the foaming process. Nevertheless, the surface nature of material substrates, including the roughness and density of polar groups, plays a key role in the multilayer growth. Hence, it is not easy to deposit a flame-retardant coating on a nonpolar EPS substrate in the beginning.[33] Therefore, the flame-retardant technology for EPS foam is another urgent issue.

According to the results and discussions aforementioned, to develop efficient flame retardants based on synergistic combinations of multiple elements and a simple and efficient flame-retardant technology, a novel phosphorus−nitrogen−silicon flame retardant based on DOPO in conjunction with a nanofiller is designed to endow it with improved flame-retardant performance through a simple surface-coating method. It endows DOPO to act either in the gas phase via flame inhibition or in the condensed phase via char formation simultaneously. As one of the representative nanofillers, the presence of potassium salt impurities and the laminated structure with ultrahigh specific surface areas make graphene oxide (GO) become highly flammable.[34]

The flame retardant for bulk polymer composites requires higher loading than a coated one because it is diluted by the polymer matrix.[35] For the flame-retardant surface-coating method we proposed, the adhesive between flame retardants and EPS foams is a newly developed phenolic epoxy resin (PER); it exhibits good heat resistance, inherent fire resistance, and high mechanical performance as well as suitable curing process in comparison with the thermosetting phenolic resins[36] and epoxy resins.[37] The developed phosphorus−nitrogen−silicon flame retardant based on DOPO further decorated with GO can solve reagglomeration of GO and migration of DOPO in the polymer matrix. Their synergistic effects can significantly give EPS foam plates an excellent flame-retardant performance.

## RESULTS AND DISCUSSION

**Chemical Structure of KDOPO and DGO.** Typical characteristic Fourier transform infrared (FT-IR) absorptions show the successful modifications of both DOPO with KH550 (Figure 1a) and KH550-modified DOPO (KDOPO) with GO (Figure 1b). The characteristic absorption bands of DOPO[38−40] and KH550[41] are summarized in Table 1. After DOPO is modified with KH550, the absorption peak of KDOPO at 2433 $cm^{-1}$, which is associated with P−H, significantly disappears. Besides, some characteristic bands associated with DOPO and KH550, such as P═O (1287 $cm^{-1}$), P−Ph (1430 $cm^{-1}$) and P−O−Ph (1139 and 1097



DOI: 10.1021/acsomega.9b03541
ACS Omega 2020, 5, 799−807

**Table 1. Functional Absorption Bands of DOPO, KH550, and GO in FT-IR**

| | functional groups | adsorption bands ($cm^{-1}$) |
|---|---|---|
| DOPO | P−H | $\nu$ 2433 |
| | phenyl | $\nu$ 1587, 1468 |
| | P−phenyl | $\delta$ 1433 |
| | P═O | $\nu$ 1238 |
| | P−O−phenyl | $\nu$ 1076, 1000 |
| KH550 | N−H | $\nu$ 3378, $\delta$ 1566 |
| | Si−O | $\nu$ 1042 |
| | $-CH_3$ | $\nu$ 2930 |
| | $-CH_2-$ | $\nu$ 2874 |
| GO | C═O | $\nu$ 1727 |
| | C═C | $\nu$ 1629 |
| | C−O−C | $\nu$ 1398 |
| | C−OH | $\nu$ 1056 |

$cm^{-1}$) functional groups, $-CH_3$ (2943 $cm^{-1}$), $-CH_2-$ (2881 $cm^{-1}$), and Si−O (1028 $cm^{-1}$) can still be found in the FT-IR spectrum of KDOPO. These results illustrate that the P−H groups of DOPO have reacted with $NH_2$ groups of KH550 and that KDOPO has been prepared successfully. The oxygen-containing functional groups indicating GO are summarized in Table 1.[42,43] After KDOPO is modified with GO, some typical absorption peaks of oxygen-containing groups, O−H stretching vibration (3048 $cm^{-1}$), C═O stretching vibration (1727 $cm^{-1}$), C═C stretching vibration (1629 $cm^{-1}$), and C−O−C stretching vibration (1398 $cm^{-1}$) are presented. These results illustrate that KDOPO-modified GO (DGO) has been prepared successfully.

X-ray diffraction (XRD) and Raman spectra also are applied to prove the success in the functionalization of DOPO. Figure 1c shows the XRD patterns of GO, DOPO, KDOPO, and DGO. The characteristic diffraction peaks of DGO present the characteristic diffraction peak of GO located at $2\theta$ = 11.6°, corresponding to the (002) reflection of GO[20] and the characteristic diffraction peak of KDOPO located at $2\theta$ = 21.6°. Figure 1d presents the Raman spectra of GO and DGO. Both samples show the existence of D and G bands at 1351 and 1603 $cm^{-1}$, respectively. In general, the intensity ratio of D to G bands ($I_D/I_G$) monitors the disordered structure and defects inside the nanocarbon and hence provides implication for the functionalization status of nanocarbons. $I_D/I_G$ for DGO increases from 0.59 to 0.76, and the XRD pattern information of DGO indicates chemical modification success between KDOPO and GO.

**Microstructure and Thermal Behavior of KDOPO and DGO.** The microstructure also reveals that DOPO presents a flat and smooth surface (Figure 2a). Relatively rough morphological features are observed for KDOPO (Figure 2b). A tight interface between KDOPO and GO can continually be observed (Figure 2d).

Thermogravimetric analysis (TGA) and differential thermogravimetric (DTG) curves of DOPO, KDOPO, and DGO composites under the nitrogen atmosphere are shown in Figure 3. As can be seen, although the degradation of KDOPO and DGO occurs earlier than DOPO, with multi decomposition steps, the degradation rate is relatively slower than that of DOPO at the same temperature. The temperature at a maximum mass loss ($T_{max}$) of DOPO is at 349.8 °C. In comparison with DOPO, $T_{max}$ of DGO increases from 349.8 to 494.9 °C. The char residues of DOPO at 800 °C are nearly 0

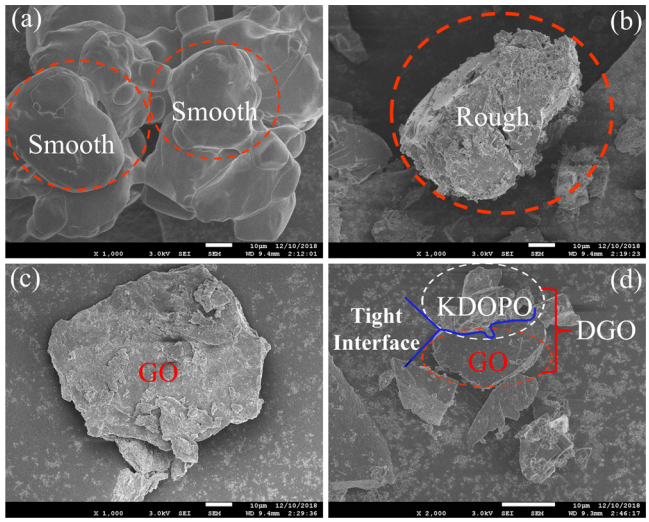


**Figure 2.** Microstructure of DOPO (a), KDOPO (b), GO (c), and DGO (d).

wt %. So, the fire-retardant mechanism of DOPO only attributes to the gas-phase fire retardancy. Significantly, DGO can obviously improve the char yield with 28.7 wt % char residues at 800 °C. Obviously, DGO can act either only in the gas phase via flame inhibition or in the condensed phase (via char formation) with synergistic combination of silicon, phosphorus, and nitrogen simultaneously.

**Flame Retardance and Combustion Behavior of EPS@DOPO and EPS@DGO.** Table 2 shows the synergistic effects of DGO on the limiting oxygen index (LOI) value and UL-94 rating for EPS@DGO foam plates. As listed in Table 2, the presence of the highest amount of DOPO (20 wt %) does not significantly improve the LOI value (LOI = 26%), whereas by substituting 10 wt % DGO in the EPS@DGO10 sample, the LOI value could be the same as EPS@DOPO20. Furthermore, V-0 rating can be easily obtained when the loading of DGO is more than 15 wt %, and the LOI value increases to greater than 28%. These results reflect the synergistic effect of the P−N−Si integrated flame retardant (DGO) on the EPS@DGO foam plate.

Digital photos of the external residues collected after the cone calorimeter test (CCT) for EPS@DOPO and EPS@DGO foam plates are portrayed in Figure 4. It can be observed that the neat EPS left nothing, and the char residues of EPS@DOPO is little and poor in expansibility. In contrast, rigid and well-expanded char residues are formed for EPS@DGO. The mass of char residues is increased by loading DGO. Actually, this rigid char layer acts as a protective shield resulting in improvement of flame-retardant performance of EPS foam plates.

CCT is still one of the most important and useful standard tests for assessing flammability as it is directly related to the actual fire situation, and the corresponding parameters are shown in Figure 5 and Table 3. It is seen that EPS foam plate burns rapidly after super short ignition time ($T_{ign}$) of 3 s with a peak heat release rate (PHRR) of 493.9 $kW/m^2$ and a total heat release (THR) of 74.32 $MJ/m^2$ at the end of the test. When the flame-retardant paintcoat, which like a protective clothing for EPS foam plate, is coated on the surface of EPS, the PHRR and THR of EPS@DOPO and EPS@DGO foam plates are significantly reduced below those of EPS foam plates. Significantly, DGO/PER paintcoat has excellent flame-


DOI: 10.1021/acsomega.9b03541
ACS Omega 2020, 5, 799−807

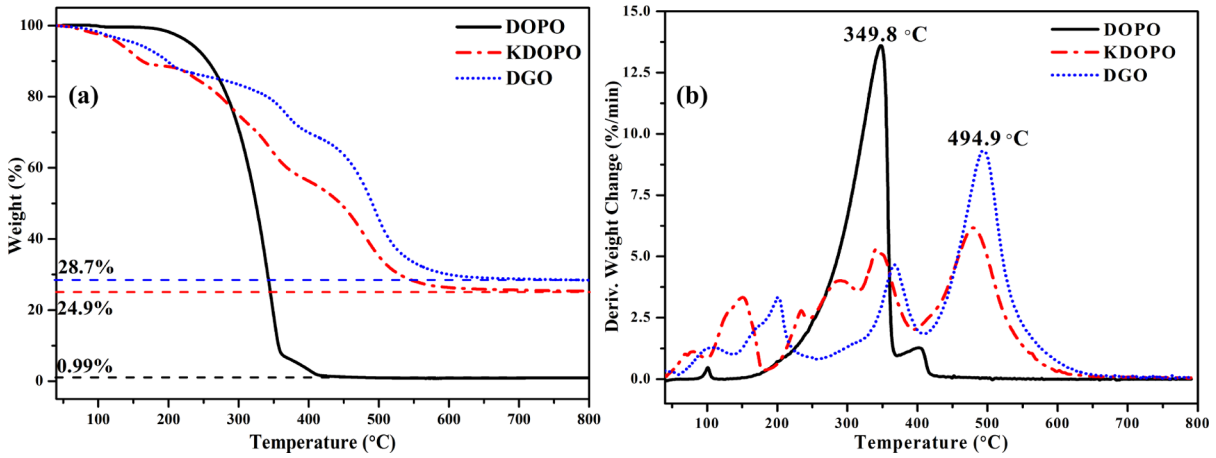


**Figure 3.** TGA (a) and DTG (b) curves versus temperature for DOPO, KDOPO, and DGO.

**Table 2. Flammability Test Results for EPS@DGO Foam Plates**

| sample | LOI (%) | drop | cotton ignited | UL-94 |
|---|---|---|---|---|
| EPS | 18 | yes | yes | fail |
| EPS@DOPO10 | 22 | yes | yes | V-2 |
| EPS@DOPO15 | 25 | yes | no | V-1 |
| EPS@DOPO20 | 26 | yes | no | V-1 |
| EPS@DGO10 | 26 | yes | no | V-1 |
| EPS@DGO15 | 28 | no | no | V-0 |
| EPS@DGO20 | 29 | no | no | V-0 |

retardant property than the DOPO/PER paintcoat with the same flame-retardant loading.

It is worth highlighting that EPS@DGO20 performs the best in enhancing the flame retardancy and exhibits the largest reduction in the PHRR and THR among the above paintcoat loadings, and PHRR and THR are reduced to 304.6 kW/m$^2$ and 39.9 MJ/m$^2$, respectively. Equivalently, PHRR and THR of EPS@DGO20 are reduced by 38.4 and 46.3%, respectively, compared with those of EPS, and reduced by 6.2 and 18.2% compared with those of EPS@DOPO20. The results indicate that the formation of an effective char layer during combustion can act as an insulating barrier between fire and the polymer matrix, which can prevent the exchange of heat and flammable gases. Moreover, the fire performance index (FPI), defined as the ratio of PHRR to $T_{ign}$, also characterizes an indication of flashover property. Generally, the lower the ratio, the lower the flashover propensity.[13,14] Table 3 indicates that FPI of EPS@DGO20 significantly decreases to 9.8 and dramatically reduces by 94.0 and 30.5% in comparison with those of EPS and EPS@DOPO20 foam plates. These results indicate that the DGO/PER flame retardant can produce less fire hazards and provide a longer evacuation time in case of fire.

The smoke released from the combustion of materials is also one of the most significant factors as most of casualties in fires are caused by asphyxia. The dynamic smoke production behaviors of EPS@DOPO and EPS@DGO foam plates are characterized by the smoke release rate (RSR) and the total smoke rate (TSR) as shown in Figures 5c,d. P-RSR and TSR of EPS@DGO20 are 16.2 s$^{-1}$ and 1794.5 m$^2$/m$^2$, which reduce by 61.3 and 62.9%, in comparison with those of neat EPS and reduce by 7.4 and 12.2% in comparison with those of EPS@DOPO20, respectively. These results indicate that the DGO flame retardant can more effectively act as the smoke

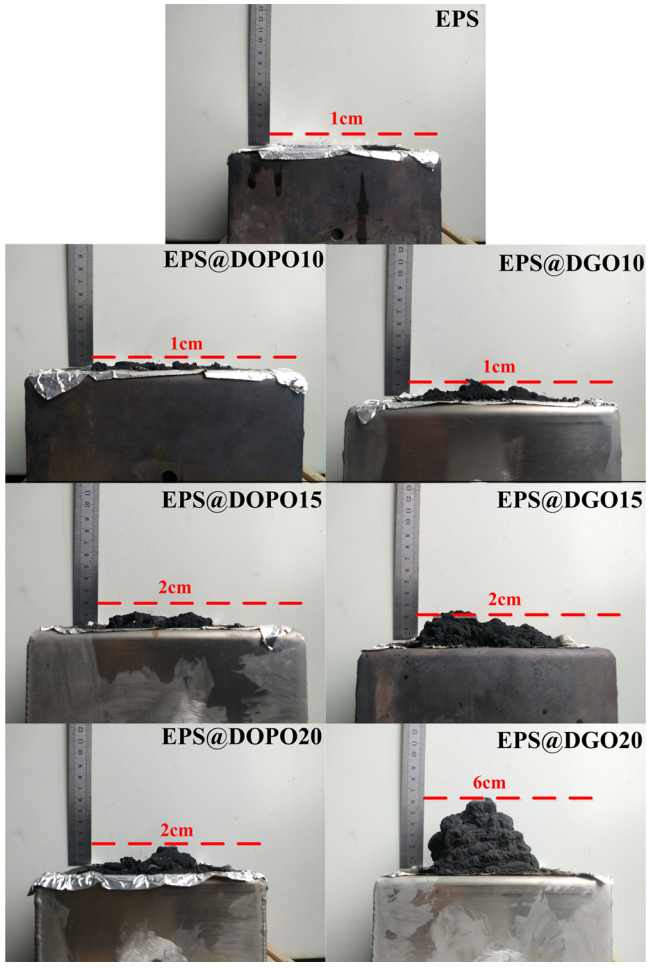


**Figure 4.** Digital images of char residues of EPS@DOPO and EPS@DGO foam plates after CCT.

suppression agent because of the synergistic flame-retardant effects of P−N−Si integrated elements in DGO and can obviously increase the chances of survival than DOPO.

Scanning electron microscopy (SEM) photographs of char residues of EPS@DOPO and EPS@DGO after CCTs are shown in Figure 6. The char residues formed from EPS@DOPO display a discontinuous and loose morphology, some large holes, probably due to the rapid release of degradation


DOI: 10.1021/acsomega.9b03541
ACS Omega 2020, 5, 799−807

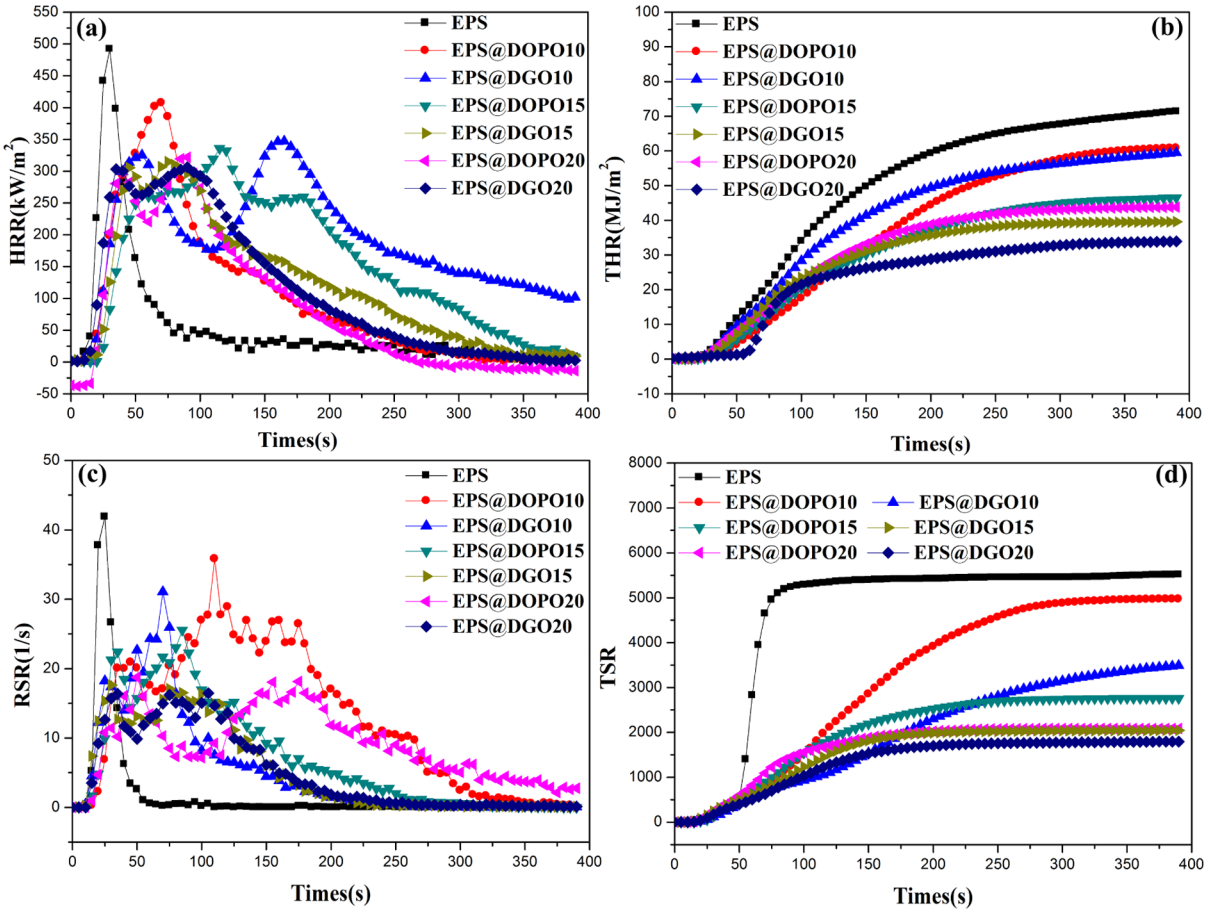


**Figure 5.** CCT results of EPS@DOPO and EPS@DGO foam plates under an external heat flux of 35 kW $m^{-2}$, (a) HRR, (b) THR, (c) RSR, and (d) TSR.

**Table 3. Characteristic Parameters of CCT Results of EPS@DOPO and EPS@DGO**

| sample | EPS | EPS@ DOPO10 | EPS@ DGO10 | EPS@ DOPO15 | EPS@ DGO15 | EPS@ DOPO20 | EPS@ DGO20 |
|---|---|---|---|---|---|---|---|
| $T_{ign}$ (s) | 3 | 10 | 15 | 21 | 23 | 23 | 31 |
| PHRR (kW/$m^2$) | 493.9 ± 2.5 | 408.7 ± 3.9 | 353.5 ± 2.6 | 339.3 ± 3.3 | 317.3 ± 4.6 | 324.6 ± 3.5 | 304.6 ± 2.8 |
| PHRR/$T_{ign}$ [kW/($m^2$/s)] | 164.6 | 40.9 | 23.6 | 16.2 | 13.8 | 14.1 | 9.8 |
| THR (MJ/$m^2$) | 74.32 ± 3.2 | 64.9 ± 2.7 | 62.8 ± 1.9 | 51.7 ± 2.6 | 45.2 ± 2.5 | 48.8 ± 3.4 | 39.9 ± 1.8 |

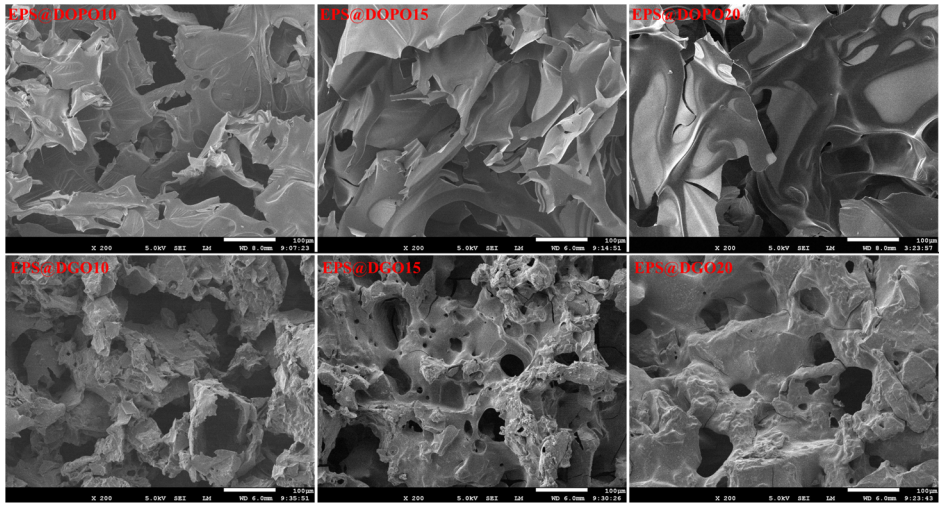


**Figure 6.** SEM images of char residues after the CCT test.



DOI: 10.1021/acsomega.9b03541
*ACS Omega* 2020, 5, 799−807

products in a short time, and large cracks, probably due to the low strength of the char residue layer. Thus, the char residue layers of EPS@DOPO could not provide an effective barrier for the underlying materials during combustion. Compared with the char morphology of EPS@DOPO foam plates, a more compact and continuous microstructure is formed for EPS@DGO foam plates, and relatively less holes can be found. The reason for this phenomenon is the relatively slower release of volatile gases during thermal degradation and the higher charring ability of DGO/PER than EPS@DOPO. Increasing the loading of DGO further leads to the formation of a more tight and thick framework on the surface of the char as well as fewer and smaller holes. These analyses are consistent with the results of the digital images of the char residues as shown in Figure 4. Both mass and heat transfers can be impeded by the more compact char layer, which is responsible for the better flame retardancy of EPS@DGO foam plates. A strong microstructure with tiny pores indicates that the existence of GO in DGO is conducive to the enhancement of strength of char residues.

**Thermal Behavior of EPS@DOPO and EPS@DGO.** Compared to that of EPS foam plate, thermal conductivity of EPS@DOPO and EPS@DGO foam plates expresses not much increase, as shown in Figure 7, even though when the DGO content is as high as 20 phr, the thermal conductivity of EPS@DGO20 just increases to 0.047 $Wm^{-1}$ $K^{-1}$ by 6.8%. It does not obviously deteriorate the thermal insulation property.[44]

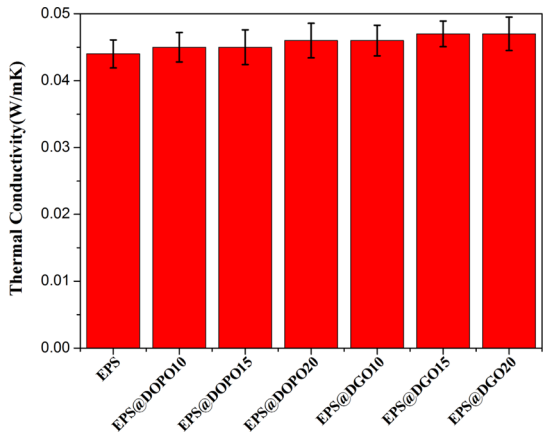


**Figure 7.** Thermal conductivity of EPS and EPS@APP foam plates.

**Flame-Retardant Mechanism.** Flame-retardant mechanism is crucial for a flame-retardant system because the mechanism is clearly studied in order to better deploy the flame-retardant system. The flame-resistance mechanism of the DGO/PER paintcoat system is proposed in Figure 8.

The reason might be related to the gas-phase and condensed-phase synergitic flame-retardant mechanisms of PER and DGO. Phosphorus-containing compounds in DGO catalyze char formation in the condensed phase and/or release small low-energy radicals (PO*) to capture active radicals in the gas phase.[17] A further formed positive silica layer in the condensed phase protects the matrix against degradation based on silicon-containing compounds in DGO.[17] Nitrogenous compounds in DGO generate inert gases that can dilute the combustible materials and heat in the flame.[45] Another indispensable flame-retardant factor can be attributed to the GO sheet in DGO. GO sheet in DGO can form a "tortuous path" and effectively retard the release rate of the volatile products (Figure 8).[46,47] Moreover, GO sheet could enhance the strength of char layers to form a strong and compact char layer.[48] The formed strong and compact char layer not only isolates the underlying matrix from the external combustible gases and thermal feedback and hinders the escape of pyrolysis volatile gases but also restricts the motion of the polymer melts,[49] which is beneficial for enhancing the antidripping properties of EPS foam plates; additionally, the barrier and reinforced effects of GO sheets play a crucial role in imparting antidripping properties to EPS foam plates.[50]

## EXPERIMENTAL DETAILS

**Materials.** EPS beads, with a granule size of 0.9−1.4 mm, were an industrial product of King Pearl Non-Modified EPS Co., Ltd, China. PER (type is F-44-80) was supplied by Marine Chemical Research Institute, China. Low-molecular-weight polyamide curing agent (SY-H115: the amine value is 220 ± 25 mgKOH/g and AHEW is 180) was supplied by Marine Chemical Research Institute, China. DOPO was generously supplied by Shandong He Zhan Chemical Co., Ltd, China. GO (9 mg/mL) was supplied by Changzhou Sixth Element Co. Ltd. (China). γ-Aminopropyltriethoxysilane (KH550) was purchased from Sigma-Aldrich Technology Co., LTD (China).

**Preparation of EPS Foam Plates.** The original EPS beads were pre-expanded in an expansion apparatus (steam oven) at

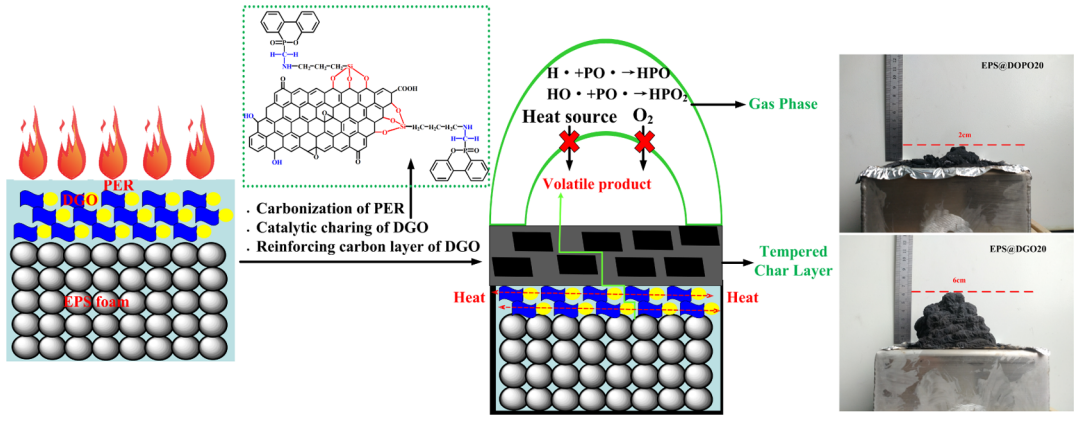


**Figure 8.** Schematic illustration of the DGO flame-retardant mechanism.



DOI: 10.1021/acsomega.9b03541
ACS Omega 2020, 5, 799−807

Scheme 1. Preparation Process for Flame-Retarded EPS@DGO Foam Plates

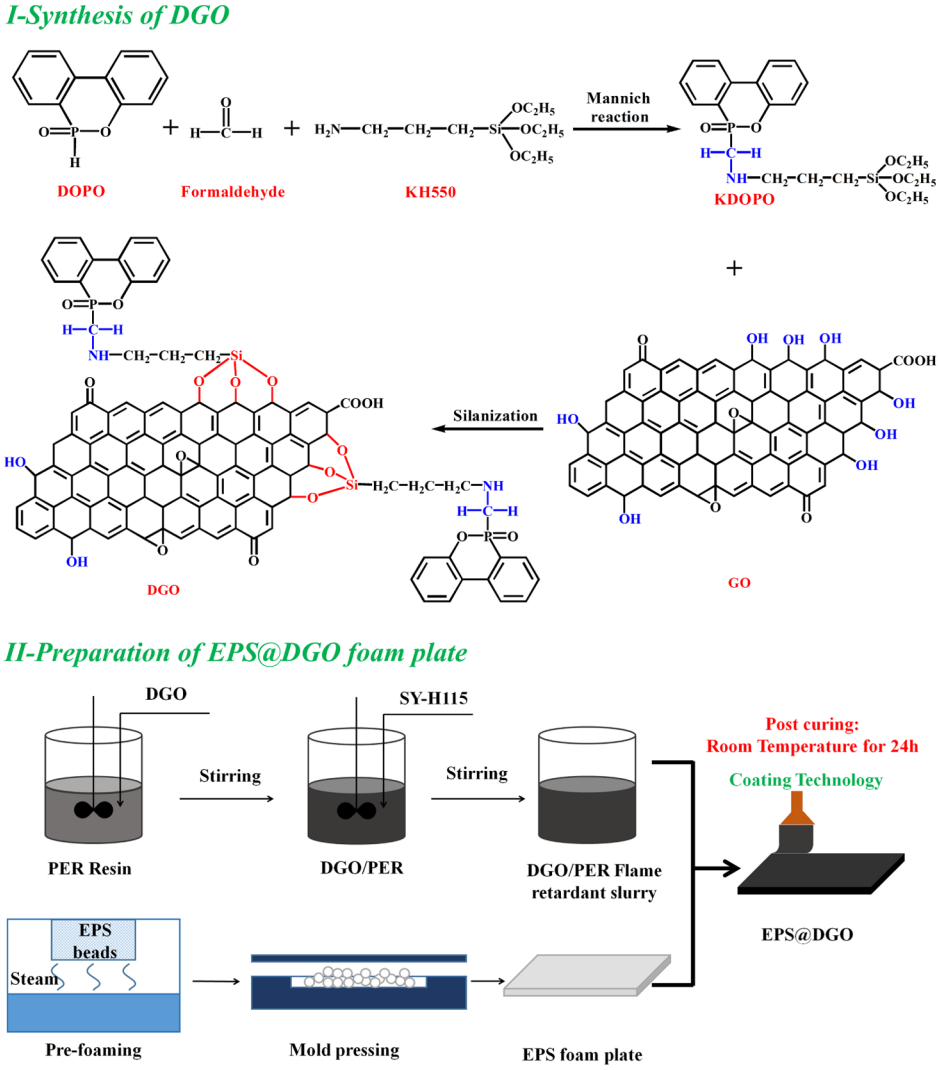


90 °C for 5 min. The pre-expanded EPS beads were aged for 24 h before use. Pre-expanded EPS beads with a foaming ratio of 40−60 can be obtained. After that, the pre-expanded EPS beads were pressed in a compression molding machine (George Moore press, UK) at 120 °C for 5 min and $3.94 \times 10^4$ kg/m$^2$ ram dia pressure. The obtained EPS foam plates were removed when the mold was cooled to room temperature.

**Preparation of DGO Flame Retardant.** DOPO (0.05 mol) was added into a vial containing 30 mL of tetrahydrofuran and then heated to 40 °C and stirred until complete dissolution. Then, 11.68 mL of KH550 (0.05 mol) and 1.84 mL of formaldehyde (0.05 mol) were added to the mixture and heated to 70 °C with mild stirring for 1 h according to Mannich reaction, and KDOPO was prepared. Subsequently, 60 mL of GO slurry (9 mg/mL) was reacted with KDOPO tetrahydrofuran solution at 50 °C for 30 min according to silanization.[51,52] Finally, the mixture was cooled to room temperature and centrifuged with 9000 rpm for 10 min to remove the supernatant liquid product. DGO was obtained after drying in a vacuum oven under 60 °C for 48 h.

**Preparation of DGO/PER Compound Flame Retardant.** DGO (10 g) was dispersed into 12 mL of ethanol solution and then mechanically mixed for 30 min. Subsequently, 20 g of PER and 12 g of SY-H115 were added to the DGO mixture with stirring. A stable and compatible inorganic−organic hybrid binder (DGO/PER) was prepared followed by these steps. For comparison, the reference sample of DOPO/PER compound flame retardant binder was prepared by the same process.

**Preparation of EPS@DOPO and EPS@DGO Foam Plates.** The process to produce flame-retarded EPS@DGO foam plates is illustrated in Scheme 1. The formulation is summarized in Table 4. The surface of EPS foam plates was coated with the calculated amount of DGO/PER flame

Table 4. Formulations of EPS@DOPO and EPS@DGO Foam Plates

| sample | PER/g | SY-H115/g | DOPO/g | DGO/g |
|---|---|---|---|---|
| EPS | 0 | 0 | 0 | 0 |
| EPS@DOPO10 | 20 | 12 | 10 | 0 |
| EPS@DOPO15 | 20 | 12 | 15 | 0 |
| EPS@DOPO20 | 20 | 12 | 20 | 0 |
| EPS@DGO10 | 20 | 12 | 0 | 10 |
| EPS@DGO15 | 20 | 12 | 0 | 15 |
| EPS@DGO20 | 20 | 12 | 0 | 20 |



DOI: 10.1021/acsomega.9b03541
ACS Omega 2020, 5, 799−807

retardant binder until a homogeneous physical blocking layer was formed after coating twice. Finally, EPS@DGO foam plates with a thin physical barrier layer were postcured at room temperature for 24 h. For comparison, the reference sample of EPS@DOPO was prepared by the same process.

**Characterization.** FT-IR spectra were recorded with a Bruker Tensor 27 spectrometer (Bruker, Germany) using the attenuated total reflectance model with a resolution of 4 $cm^{-1}$ and 32 scans. Ultraviolet−visible (UV−vis) spectra were performed on a TU-1901PC spectrophotometer. XRD pattern was recorded on a Rigaku D-MAX2500-PC diffractometer. Raman spectra were recorded using a high-resolution FRS-100S (Bruker, Germany) machine with a CCD detector. The spectral purity was quoted to be <700 at a wavelength >2100 $cm^{-1}$ from a set wavelength. The morphology of char residues was observed using a JSM-6700F (Japan Electronics Corp.) microscope. TGA measurement was carried out using a TGA-7 type thermo-analysis instrument (Perkine Elmer Company, USA) from room temperature to 800 °C at a heating rate of 10 °C/min under a $N_2$ atmosphere. LOI was measured using a HC-2 oxygen index meter (Jiangning Analysis Instrument Company, China). UL-94 vertical burning test was performed on a vertical burning instrument (CFZ-1 type, Jiangning Analysis Instrument Co., China). The CCT was performed on the cone calorimeter (Fire Testing Technology, U.K.). Each specimen was wrapped in an aluminum foil and exposed horizontally to 50 $kW/m^2$ external heat flux.

## CONCLUSIONS

The aim of our study was to investigate synergistic high flame-retardant EPS foam plates through an effective protective surface-coating method. Considering its convenient operation and high efficiency, the facile method was developed to construct P−N−Si integrated flame-retardant (DGO) paint-coat based on PER in EPS foam plates. The LOI values of EPS@DGO15 and EPS@DGO20 foam plates increased, respectively, up to 28 and 29%, and a V-0 rating for them was achieved. Besides, P-RSR and TSR of EPS@DGO20 were 16.2 $s^{-1}$ and 1794.5 $m^2/m^2$, which reduced by 61.3 and 62.9% in comparison with those of neat EPS and reduced by 7.4 and 12.2% in comparison with those of EPS@DOPO20. FPI of EPS@DGO20 significantly decreased to 9.8 and dramatically reduced by 94.0 and 30.5% in comparison with those of EPS and EPS@DOPO20. These results indicated that the DGO/PER flame-retardant paintcoat produced less fire hazards and provided a longer evacuation time in case of fire to effectively develop flame-retardant ability and improved significantly fire safety of EPS foam plates in buildings and constructions, thereby importantly reducing the secondary disaster induced by fire without deteriorating the thermal insulation performance of EPS foam plates.

## AUTHOR INFORMATION


### Corresponding Authors

*E-mail: qustlilin@163.com (L.L.).
*E-mail: lyzhsh@163.com (S.Z.).

### ORCID

Lin Li: 0000-0001-9754-7536
Shuai Zhao: 0000-0003-2115-4378

### Author Contributions

†L.L. and X.S. contributed equally to this work and should be considered co-first authors.


### Notes

The authors declare no competing financial interest.

## ACKNOWLEDGMENTS

The authors gratefully acknowledge the support from the National Natural Science Foundation of China (grant numbers 51603111 and 51703111), the Natural Science Foundation of Shandong Province, China (grant numbers 2018GGX102015 and ZR2017BEM011), and the China Postdoctoral Science Foundation (grant number 2018M642626).

## REFERENCES


(1) Demirel, B. Optimization of the composite brick composed of expanded polystyrene and pumice blocks. *Constr. Build. Mater.* **2013**, *40*, 306−313.
(2) Raps, D.; Hossieny, N.; Park, C. B.; Altstädt, V. Past and present developments in polymer bead foams and bead foaming technology. *Polymer* **2015**, *56*, 5−19.
(3) Schellenberg, J.; Wallis, M. Dependence of properties of expandable polystyrene particle foam on degree of fusion. *J. Appl. Polym. Sci.* **2010**, *115*, 2986−2990.
(4) Hong, Y.; Fang, X.; Yao, D. Processing of composite polystyrene foam with a honeycomb structure. *Polym. Eng. Sci.* **2015**, *55*, 1494−1503.
(5) Wang, S.; Chen, H.; Liu, N. Ignition of expandable polystyrene foam by a hot particle: An experimental and numerical study. *J. Hazard. Mater.* **2015**, *283*, 536−543.
(6) Hiebl, J.; Vetter, W. Detection of hexabromocyclododecane and its metabolite pentabromocyclodedecane in chicken egg and fish from the official food control. *J. Agric. Food Chem.* **2007**, *55*, 3319−3324.
(7) Covaci, A.; Gerecke, A. C.; Law, R. J.; Voorspoels, S.; Kohler, M.; Heeb, N. V.; Leslie, H.; Allchin, C. R.; De Boer, J. Hexabromocyclododecanes (HBCDs) in the environment and humans: a review. *Environ. Sci. Technol.* **2006**, *40*, 3679−3688.
(8) Shaw, S. D.; Blum, A.; Weber, R.; Kannan, K.; Rich, D.; Lucas, D.; Koshland, C. P.; Dobraca, D.; Hanson, S.; Birnbaum, L. S. Halogenated flame retardants: do the fire safety benefits justify the risks? *Rev. Environ. Health* **2010**, *25*, 261−305.
(9) Shi, Y.; Yu, B.; Zheng, Y.; Yang, J.; Duan, Z.; Hu, Y. Design of reduced graphene oxide decorated with DOPO phosphanomidate for enhanced fire safety of epoxy resin. *J. Colloid Interface Sci.* **2018**, *521*, 160−171.
(10) Zhao, S.; Xie, S.; Zhao, Z.; Zhang, J.; Li, L.; Xin, Z. Green and high-efficiency production of graphene by tannic acid assisted exfoliation of graphite in water. *ACS. Sustain. Chem. Eng.* **2018**, *6*, 7652−7661.
(11) Zhao, Z.; Li, L.; Shao, X.; Liu, X.; Zhao, S.; Xie, S.; Xin, Z. Tannic acid-assisted green fabrication of functionalized graphene towards its enhanced compatibility in NR nanocomposite. *Polym. Test.* **2018**, *70*, 396−402.
(12) Liu, G.; Chen, W.; Yu, J. A novel process to prepare ammonium polyphosphate with crystalline form II and its comparison with melamine polyphosphate. *Ind. Eng. Chem. Res.* **2010**, *49*, 12148−12155.
(13) Shao, Z.-B.; Deng, C.; Tan, Y.; Yu, L.; Chen, M.-J. polyphosphate chemically-modified with ethanolamine as an efficient intumescent flame retardant for polypropylene. *J. Mater. Chem. A* **2014**, *2*, 13955−13965.
(14) Schartel, B.; Hull, T. R. Development of fire-retarded materials-interpretation of cone calorimeter data. *Fire Mater.* **2007**, *31*, 327−354.
(15) Chen, S.; Li, X.; Li, Y.; Sun, J. Intumescent flame retardant and self-healing superhydrophobic coatings on cotton fabric. *ACS Nano* **2015**, *9*, 4070−4076.
(16) Kandola, B. K.; Horrocks, A. R. Complex char formation in flame-retarded fibre-intumescent combinations-ii thermal analytical studies. *Polym. Degrad. Stab.* **1996**, *54*, 289−303.




DOI: 10.1021/acsomega.9b03541
*ACS Omega* 2020, 5, 799−807

(17) Köklükaya, O.; Carosio, F.; Grunlan, J. C.; Wagberg, L. Flame-retardant paper from wood fibers functionalized via layer-by-layer assembly. *ACS Appl. Mater. Interfaces* **2015**, *7*, 23750−23759.
(18) Schartel, B.; Braun, U.; Balabanovich, A. I.; Artner, J.; Ciesielski, M.; Döring, M.; Perez, R. M.; Sandler, J. K. W.; Altstädt, V. Pyrolysis and fire behaviour of epoxy systems containing a novel 9,10-dihydro-9-oxa-10-phosphaphenanthrene-10-oxide-(DOPO)-based diamino hardener. *Eur. Polym. J.* **2008**, *44*, 704−715.
(19) Qian, X.; Song, L.; Bihe, Y.; Yu, B.; Shi, Y.; Hu, Y.; Yuen, R. K. K. Organic/inorganic flame retardants containing phosphorus, nitrogen and silicon: Preparation and their performance on the flame retardancy of epoxy resins as a novel intumescent flame retardant system. *Mater. Chem. Phys.* **2014**, *143*, 1243−1252.
(20) Guo, W.; Yu, B.; Yuan, Y.; Song, L.; Hu, Y. In situ preparation of reduced graphene oxide/DOPO-based phosphonamidate hybrids towards high-performance epoxy nanocomposites. *Compos. B Eng.* **2017**, *123*, 154−164.
(21) Neisius, N. M.; Lutz, M.; Rentsch, D.; Hemberger, P.; Gaan, S. Synthesis of DOPO-based phosphonamidates and their thermal properties. *Ind. Eng. Chem. Res.* **2014**, *53*, 2889−2896.
(22) Salmeia, K. A.; Gaan, S. An overview of some recent advances in DOPO derivatives: chemistry and flame retardant applications. *Polym. Degrad. Stab.* **2015**, *113*, 119−134.
(23) Zhao, P.; Liu, S.; Xiong, K.; Wang, W.; Liu, Y. Highly flame retardancy of cotton fabrics with a novel phosphorus/nitrogen/silicon flame-retardant treating system. *Fibers Polym.* **2016**, *17*, 569−575.
(24) Zhu, Z.-M.; Xu, Y.-J.; Liao, W.; Xu, S.; Wang, Y.-Z. Highly flame retardant expanded polystyrene foams from phosphorus-nitrogen-silicon synergistic adhesives. *Ind. Eng. Chem. Res.* **2017**, *56*, 4649−4658.
(25) Chao, P.; Li, Y.; Gu, X.; Han, D.; Jia, X.; Wang, M.; Zhou, T.; Wang, T. Novel phosphorus-nitrogen-silicon flame retardants and their application in cycloaliphatic epoxy systems. *Polym. Chem.* **2015**, *6*, 2977−2985.
(26) Wu, D.; Zhao, P.; Zhang, M.; Liu, Y. Preparation and properties of flame retardant rigid polyurethane foam with phosphorus-nitrogen intumescent flame retardant. *High Perform. Polym.* **2013**, *25*, 868−875.
(27) Chen, X.; Liu, Y.; Bai, S.; Wang, Q. Macromolecular nitrogen-phosphorous compound/expandable graphite synchronous expansion flame retardant polystyrene foam. *Polym.-Plast. Technol. Eng.* **2014**, *53*, 1402−1407.
(28) Wang, L. Y.; Wang, C.; Liu, P. W.; Jing, Z. J.; Ge, X. S.; Jiang, Y. J. The flame resistance properties of expandable polystyrene foams coated with a cheap and effective barrier layer. *Constr. Build. Mater.* **2018**, *176*, 403−414.
(29) Zhu, Z.-M.; Xu, Y.-J.; Liao, W.; Xu, S.; Wang, Y.-Z. Highly flame retardant expanded polystyrene foams from phosphorus-nitrogen-silicon synergistic adhesives. *Ind. Eng. Chem. Res.* **2017**, *56*, 4649−4658.
(30) Kandola, B. K.; Krishnan, L.; Ebdon, J. R. Blends of unsaturated polyester and phenolic resins for application as fire-resistant matrices in fire-reinforced composites: effects of added flame retardants. *Polym. Degrad. Stab.* **2014**, *106*, 129−137.
(31) Zhang, D.; Williams, B. L.; Becher, E. M. retardant and hydrophobic cotton fabrics from intumescent coatings. *Adv. Compos. Hybrid Mater.* **2018**, *1*, 177−184.
(32) Mehra, N.; Jeske, M.; Yang, X.; Gu, J.; Kashfipour, M. A.; Li, Y.; Baughman, J. A. Hydrogen-bond driven self-assembly of two-dimensional supramolecular melamine-cyanuric acid crystals and its self-alignment in polymer composites for enhanced thermal conduction. *ACS Appl. Polym. Mater.* **2019**, *1*, 1291−1300.
(33) Richardson, J. J.; Bjornmalm, M.; CarusoMultilayer, F. Assembly, technology-driven layer-by-layer assembly of nanofilms. *Science* **2015**, *348*, aaa2491−aaa2501.
(34) Hu, W.; Yu, B.; Jiang, S.-D.; Song, L.; Hu, Y.; Wang, B. Hyperbranched polymer grafting graphene oxide as an effective flame retardant and smoke suppressant for polystyrene. *J. Hazard. Mater.* **2015**, *300*, 58−66.
(35) Jung, D.; Bhattacharyya, D. Keratinous fiber based intumescent flame retardant with controllable functional compound loading. *ACS Sustain. Chem. Eng.* **2018**, *6*, 3177−13184.
(36) Zheng, C.; Liang, S. Preparation and damping properties of medium-temperature co-cured phenolic resin matrix composite structures. *Compos. Struct.* **2019**, *217*, 122−129.
(37) Gu, J.; Yang, X.; Li, C.; Kou, K. Synthesis of cyanate ester microcapsules via solvent evaporation technique and its application in epoxy resins as a healing agent. *Ind. Eng. Chem. Res.* **2016**, *55*, 10941−10946.
(38) Tang, C.; Yan, H.; Li, M.; Lv, Q. A novel phosphorus-containing polysiloxane for fabricating high performance electronic material with excellent dielectric and thermal properties. *J. Mater. Sci. Mater. Electron.* **2018**, *29*, 195−204.
(39) Fang, Y.; Zhou, X.; Xing, Z.; Wu, Y. An effective flame retardant for poly(ethylene terephthalate) synthesized by phosphaphenanthrene and cyclotriphosphazene. *J. Appl. Polym. Sci.* **2017**, *134*, 45246.
(40) Wan, X.; Zhan, Y.; Long, Z.; Zeng, G.; He, Y. Core@double-shell structured magnetic halloysite nanotube nano-hybrid as efficient recyclable adsorbent for methylene blue removal. *Chem. Eng. J.* **2017**, *330*, 491−504.
(41) Wan, X.; Zhan, Y.; Long, Z.; Zeng, G.; Ren, Y.; He, Y. High-performance magnetic poly (arylene ether nitrile) nanocomposites: co-modification of $Fe_3O_4$ via mussel inspired poly (dopamine) and amino functionalized silane KH550. *Appl. Surf. Sci.* **2017**, *425*, 905−914.
(42) Stankovich, S.; Piner, R. D.; Nguyen, S. T.; Ruoff, R. S. Synthesis and exfoliation of isocyanate-treated graphene oxide nanoplatelets. *Carbon* **2006**, *44*, 3342−3347.
(43) Wang, X.; Song, L.; Yang, H.; Xing, W.; Kandola, B.; Hu, Y. Simultaneous reduction and surface functionalization of graphene oxide with POSS for reducing fire hazards in epoxy composites. *J. Mater. Chem.* **2012**, *22*, 22037−22043.
(44) Yang, X.; Liang, C.; Ma, T.; Guo, Y.; Kong, J.; Gu, J.; Chen, M.; Zhu, J. A review on thermally conductive polymeric composites: classification, measurement, model and equations, mechanism and fabrication methods. *Adv. Compos. Hybrid Mater.* **2018**, *1*, 207−230.
(45) Kandola, B. K.; Horrocks, A. R. Complex char formation in flame-retarded fibre-intumescent combinations II. thermal analytical studies. *Polym. Degrad. Stab.* **1996**, *54*, 289−303.
(46) Shi, Y.; Yu, B.; Zheng, Y.; Yang, J.; Duan, Z.; Hu, Y. Design of reduced graphene oxide decorated with DOPO-phosphanomidate for enhanced fire safety of epoxy resin. *J. Colloid Interface Sci.* **2018**, *521*, 160−171.
(47) Xie, H.; Lai, X.; Li, H.; Gao, J.; Zeng, X.; Huang, X.; Lin, X. A highly efficient flame retardant nacre-inspired nanocoating with ultrasensitive fire-warning and self-healing capabilities. *Chem. Eng. J.* **2019**, *369*, 8−17.
(48) Wang, X.; Xing, W.; Feng, X.; Yu, B.; Song, L.; Hu, Y. Functionalization of graphene with grafted polyphosphamide for flame retardant epoxy composites: synthesis, flammability and mechanism. *Polym. Chem.* **2014**, *5*, 1145−1154.
(49) Fan, S.; Yuan, R.; Wu, D.; Wang, X.; Yu, J.; Li, F. Silicon/nitrogen synergistically reinforced flameretardant PA6 nanocomposites with simultaneously improved anti-dripping and mechanical properties. *RSC Adv.* **2019**, *9*, 7620−7628.
(50) Wang, C.; Wu, L.; Dai, Y.; Zhu, Y.; Wang, B.; Zhong, Y.; Zhang, L.; Sui, X.; Xu, H.; Mao, Z. Application of self-templated PHMA sub-microtubes in enhancing flame-retardance and anti-dripping of PET. *Polym. Degrad. Stab.* **2018**, *154*, 239−247.
(51) Zhao, S.; Xie, S. C.; Liu, X. L.; Shao, X. M.; Zhao, Z.; Xin, Z. X.; Li, L. Covalent hybrid of graphene and silicon dioxide and reinforcing effect in rubber composites. *J. Polym. Res.* **2018**, *25*, 225.
(52) Zhao, S.; Xie, S.; Sun, P.; Zhao, Z.; Li, L.; Shao, X.; Liu, X.; Xin, Z. Synergistic effect of graphene and silicon dioxide hybrids through hydrogen bonding self-assembly in elastomer composites. *RSC Adv.* **2018**, *8*, 17813−17825.


DOI: 10.1021/acsomega.9b03541
*ACS Omega* 2020, 5, 799−807